# Capacitance cytometry: Measuring biological cells one by one

L. L. Sohn*†, O. A. Saleh*, G. R. Facer*, A. J. Beavis‡, R. S. Allan‡, and D. A. Notterman†‡

Departments of *Physics and ‡Molecular Biology, Princeton University, Princeton, NJ 08544

Communicated by Lewis T. Williams, Chiron Technologies, Emeryville, CA, August 1, 2000 (received for review May 19, 2000)

**Measuring the DNA content of eukaryotic cells is a fundamental task in biology and medicine. We have observed a linear relationship between the DNA content of eukaryotic cells and the change in capacitance that is evoked by the passage of individual cells across a 1-kHz electric field. This relationship is species-independent; consequently, we have developed a microfluidic technique—"capacitance cytometry"—that can be used to quantify the DNA content of single eukaryotic cells and to analyze the cell-cycle kinetics of populations of cells. Comparisons with standard flow cytometry demonstrate the sensitivity of this new technique.**

The electrical properties of biological cells are of great interest, as they can provide opportunities to develop novel, rapid assays for disease (1, 2) and integrated hybrid chips for electronics (3–7). Previous electrical studies of cells have focused on external macroscopic properties, such as cell membrane responses or volume, and have reflected primarily those of large ensembles of cells (8, 9). Here, we report an innovative technique we have developed recently that allows one to investigate—all on an integrated microfluidic chip—some of the internal properties of individual cells. We term this technique "capacitance cytometry." Capacitance cytometry can quantify the DNA content of single eukaryotic cells from a diverse set of organisms, ranging from yeast to mammals. In addition, capacitance cytometry can be used as an assay for abnormal changes in DNA content, such as are encountered frequently in neoplastic cells. By monitoring the DNA content of populations of cells with this technique, one can produce a profile of their cell-cycle kinetics. Thus, capacitance cytometry may, in the future, serve as a medical diagnostic tool whose low-detection limit of just one cell can identify the presence of malignancy in very small quantities of tissue, and without special processing.

Although also able to interrogate cells one by one, standard laser flow cytometry requires sample preparation such as sample staining or manipulation of cells. In contrast, our technique requires no special preparation. Thus, capacitance cytometry has the potential to be simpler, faster, and less expensive than standard laser flow cytometry.

The fundamental basis of capacitance cytometry is an AC capacitance measurement. This extremely sensitive yet robust electronic technique allows one to probe the polarization response of a wide range of materials—both organic and inorganic—to an external electric field. In the past, capacitance measurements have been used to identify and investigate a number of different materials in bulk (10). More recently, it has been used to investigate ensembles of biological cells—determining cell size and cellular membrane capacitance—to assay cell-cycle progression (8) and to differentiate normal and malignant white blood cells (9). In contrast, here we employ capacitance measurements as a means of detecting and quantifying the polarization response of DNA within the nucleus of single eukaryotic cells. Because DNA is a highly charged molecule, in an applied low-frequency AC electric field, its polarization response, in combination with the motion of the surrounding counterions, can be substantial (11–13). We measure this response as a change in total capacitance, $\Delta C_T$, across a pair of microelectrodes as individual eukaryotic cells suspended in buffer solution flow one by one through a microfluidic channel (see Fig. 1). Unlike a Coulter counter, which measures displaced volume as cells or particles flow through a small orifice (14), our integrated microfluidic chip measures the polarization response of a cell as it passes through an electric field region. The data we obtain therefore relate, at least in part, to the charge distribution within the cell.

Electronic measurements in conductive solutions often lead to complications resulting from charge-screening effects at the electrode–fluid interface, i.e., "electrode polarization." The measurements we report here are subject to these ionic effects, a fact that prevents our interpreting absolute capacitance values. However, because electrode polarization is localized to the electrode surface (to within the Debye screening length for the solution) and remains constant for a particular device geometry, ion concentration, and applied frequency, we can determine cellular properties by comparing changes in total capacitance values among different cells passing through our device.

The fabrication of our integrated microfluidic device is a multistage process. Photolithography first is used to fabricate a pair of 50-$\mu$m-wide, gold microelectrodes, constituting the sensor, onto a glass or quartz substrate. Fig. 1*a* shows a schematic of the entire device. The distance separating the two electrodes is 30 $\mu$m, three times larger than the average diameter of the eukaryotic cells we examined.[§] Millimeter-sized holes then are drilled through the substrate on either side of the completed electrodes to provide an inlet and outlet for the fluid and cells.

Once the central device has been fabricated, we use soft lithography (15) to create a polydimethyl siloxane (PDMS) microfluidic channel. To avoid complications arising from a cell passing directly over only one electrode and to minimize the effects of electrode polarization, we chose the channel width to be the distance separating the two electrodes. We used two different channel heights, $h = 30$ $\mu$m and $h = 40$ $\mu$m, in our experiments. We found that measurements made with $h = 40$ $\mu$m were lower in sensitivity than those with $h = 30$ $\mu$m but gave quantitatively similar results, up to an overall scale factor. Once we aligned and positioned the PDMS channel over the electrodes and holes (see Fig. 1*b*), we used a syringe pump (Model KD2100, KD Scientific Syringe Pump; KD Scientific, New Hope, PA) to deliver fluid to the completed device at nonpulsatile rates ranging from 1 $\mu$l/hr to 300 $\mu$l/hr.

We measure the capacitance of the completed device by using a commercial capacitance bridge (AH2500A 1-kHz Ultra-

Abbreviation: PDMS, polydimethyl siloxane.

†To whom reprint requests should be addressed at: Department of Physics, Jadwin Hall, Princeton University, Princeton, NJ 08544. E-mail: sohn@princeton.edu or dnotterman@princeton.edu.

§Smaller electrodes separated by 10 nm and fabricated by using standard electron-beam lithography can be used in similar devices to detect single biomacromolecules (O.A.S. and L.L.S., unpublished results).

The publication costs of this article were defrayed in part by page charge payment. This article must therefore be hereby marked "*advertisement*" in accordance with 18 U.S.C. §1734 solely to indicate this fact.

Article published online before print: *Proc. Natl. Acad. Sci. USA*, 10.1073/pnas.200361297. Article and publication date are at www.pnas.org/cgi/doi/10.1073/pnas.200361297

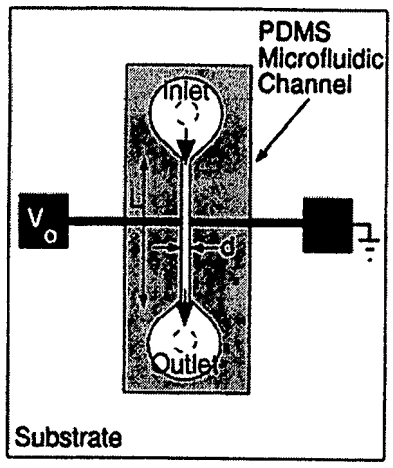


(a)

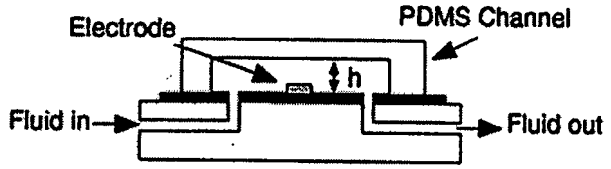


(b)

Fig. 1. Schematic illustration of the integrated microfluidic device. (*a*) Top view shows the entire device, including electrode configuration, inlet and outlet holes for fluid, and the PDMS microfluidic channel. The electrodes are made of gold and are 50 $\mu$m wide. The distance, *d*, separating the electrodes is 30 $\mu$m. The width of the PDMS microfluidic channel is also *d*, the length, *L*, is 5 mm, and the height, *h*, is either 30 $\mu$m or 40 $\mu$m. (*b*) Side view along the vertical axis of the device shows a detailed view of fluid delivery. Fluid delivery is accomplished with a syringe pump at nonpulsatile rates ranging from 1 to 300 $\mu$l/hr.

Precision Capacitance Bridge, Andeen Hagerling, Cleveland). This bridge applies a voltage ($V_{rms}$ = 250 mV) at a frequency of 1 kHz across the device.[¶] By electrically shielding the device and controlling the temperature precisely (to within ± 0.05°C), we are able to achieve noise levels of ≈5 aF when the microfluidic channel is dry and 0.1–2 fF when wet.

We have used our device to compare the DNA content of individual eukaryotic cells. Because the position of such a cell along the mitotic cell cycle is strictly related to DNA content—a cell in $G_0/G_1$ phase has 2N DNA content, a cell in $G_2$/M phase has 4N DNA content, and a cell in S phase has between 2N and 4N DNA content—we should be able to determine the phase of an individual cell. Because DNA is a highly charged molecule, we anticipate that it will produce a change in capacitance, and this change should scale approximately with the DNA content of the cell, at least at frequencies up to 1 kHz. Thus, the device response $\Delta C_T$ to a cell in $G_2$/M phase should be roughly twice that in $G_0/G_1$ phase, because the former has twice the DNA content (4N vs. 2N DNA content); the response to a cell in S phase should be between that of the $G_0/G_1$–$G_2$/M phases; and finally, the response to a hyperdiploid cell (greater than 4N DNA content) should be greater than that of either a $G_0/G_1$, S, or $G_2$/M phase cell.

[¶]A $V_{rms}$ = 250 mV is applied such that it represents a small perturbation to the entire system. At this voltage, electrolysis and dielectrophoretic trapping can be ignored because both occur at higher voltages, $V_{rms}$ > 1V. In addition, $V_{rms}$ = 250 mV produces an optimal signal-to-noise ratio for the particular capacitance bridge used.

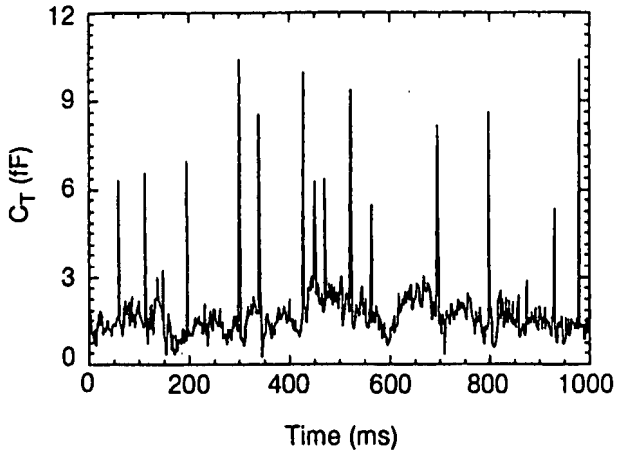


Fig. 2. Device response over a course of 1,000 ms to fixed mouse myeloma SP2/0 cells suspended in 75% ethanol/25% PBS solution at 10°C. Distinct peaks are present in the data; each peak corresponds to a single cell flowing past the electrodes. The slight difference in peak widths is an artifact of the time-resolution limit of the data acquisition. The channel height of the device was 30 $\mu$m.

Mouse myeloma cells (SP2/0), a malignant cell line, were grown in suspension to a density of approximately $10^5$ cells/ml. The cells then were washed in PBS solution (pH 7.4), fixed in 75% ethanol at −20°C for a minimum of 24 h, washed again with PBS solution, treated with RNase, and then washed and resuspended for storage in 75% ethanol. Standard analysis (FACScan flow cytometer; Becton Dickinson Immunocytometry Systems), after treatment with a nucleic acid probe (SYTOX Green Nucleic Acid Stain; Molecular Probes), showed that approximately 41% of the cells were in $G_0/G_1$ phase, 40% were in S phase, 18% were in $G_2$/M phase of the cell cycle, and <1% were hyperdiploid.

For any given experimental run, microliters of fixed cells at a concentration of $10^5$ cells/ml were injected into our device at a rate of 1 $\mu$l/hr. Using cells tagged with a fluorescent probe (SYTOX Green Nucleic Acid Stain), we visually confirmed that, at this dilute concentration, cells flowed one by one through the microfluidic channel at an average cell velocity of ≈250 $\mu$m/sec.[‖] The Reynolds number was estimated to be Re~$10^{-2}$, thus ensuring that flow in the channel was laminar.

Fig. 2 is a representative response we obtained when cells passed through a device having a channel height of 30 $\mu$m. As shown in the figure, we observed a series of sharp peaks whose amplitudes $\Delta C_T$ range from ≈3 fF to ≈12 fF. The individual peaks are separated by time intervals ranging from 40 to 100 ms. Optical observations during similar measurement runs confirmed that each peak indeed does correspond to a single cell flowing past the electrodes.

A central analysis technique in flow cytometry is the DNA histogram, which provides a visual representation of the number of cells as a function of DNA content and, therefore, the proportion of cells in each phase of the cell cycle. Fig. 3 is a histogram resulting from our capacitance measurements. As shown, there are two distinct populations of SP2/0 cells: one corresponding to 2N DNA content, centered at 12.3 fF, and one corresponding to 4N DNA content, centered at 23.0 fF. Based on this capacitance histogram, we judge that approximately 48% of the cells are in $G_0/G_1$ phase, 30% are in S phase, 22% are in $G_2$/M phase, and <1% are hyperdiploid. This distribution is comparable to that achieved with standard laser flow cytometry (Fig. 3 *Inset*).

[‖]For a movie of the cells flowing through the microfluidic channel, see http://oberon.princeton.edu.

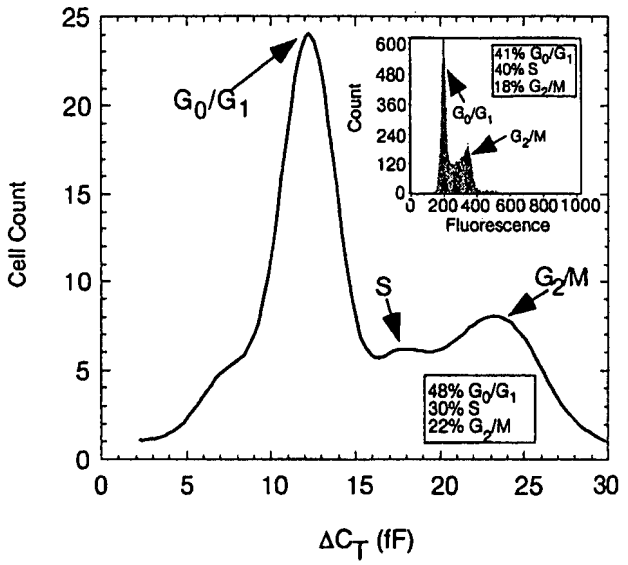


Fig. 3. Frequency histogram of the SP2/0 cells obtained with a device of $h$ = 30 $\mu$m, as compared with that obtained by conventional laser flow cytometry. The ungated histogram shows two major peaks, one centered at 12.3 fF, corresponding to $G_0/G_1$ phase, and one centered at 23.0 fF, corresponding to $G_2/M$ phase. The distribution of cells at capacitances less than 10 fF correspond to hypodiploid cells; the distribution of cells at capacitances greater than 27 fF is due to hyperdiploid cells. Based on the histogram obtained, we judged that approximately 48% are in $G_0/G_1$ phase, 30% are in S phase, and 22% are in $G_2/M$ phase. This cell cycle distribution is comparable to that obtained by conventional flow cytometry. (*Inset*) Histogram obtained via conventional flow cytometry. The data have been gated and do not include hypo- and hyperdiploid cells. Two peaks at fluorescence channels 190 and 380 correspond to $G_0/G_1$ and $G_2/M$ phases, respectively.

The histogram shown in Fig. 3 strongly suggests that our device is able to differentiate cells in different phases of the cell cycle. We can safely rule out the possibility that the measured differences in capacitance are due to cells flowing past the electrodes at different channel positions with respect to the electrodes, because we have optically confirmed that the cells flow in the center of the channel and directly between the electrodes.

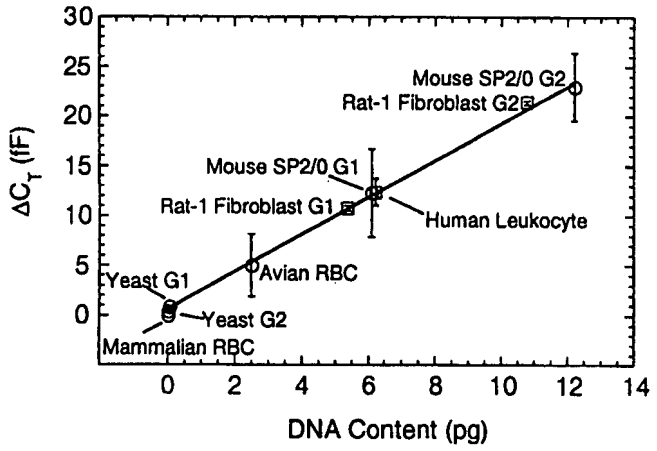


Fig. 4. Change in capacitance, $\Delta C_T$, vs. DNA content of mouse SP2/0, yeast, avian, and mammalian red blood cells. As shown, there is a linear relationship between $\Delta C_T$ and DNA content at 1-kHz frequency. O, Data taken with a device whose channel height was 30 $\mu$m; □, data taken with a device whose channel height was 40 $\mu$m. The 40-$\mu$m data were scaled by the ratio of the $\Delta C_T$ values obtained for mouse SP2/0 cells measured with 30-$\mu$m- and 40-$\mu$m-high channel devices (see ** footnote). All data were obtained at $T$ = 10°C and in PBS solution.

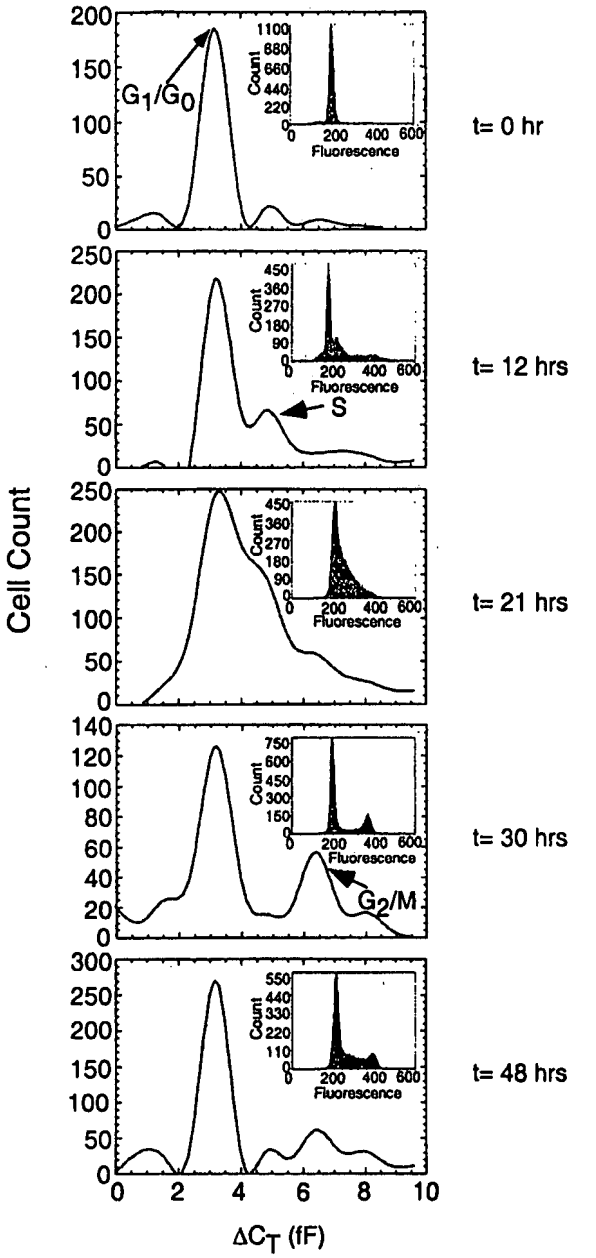


Fig. 5. DNA progression of Rat-1, rodent fibroblast cells. Cells were $G_0/G_1$ arrested ($t$ = 0 h) and then allowed to progress through one mitotic cell cycle in synchrony. At $t$ = 12 h, the cells are beginning to enter S phase, and at $t$ = 21 h, they have fully entered this phase. At $t$ = 30 h, the cells have entered $G_2/M$ phase. This is shown by the secondary peak at $\Delta C_T$ =6.4 fF. At $t$ = 48 h, the cells have completed one mitotic cell cycle and are once again in $G_0/G_1$ phase. The $G_0/G_1$, S, and $G_2/M$ phases are indicated with arrows. The data shown were taken at $T$ = 10°C with a microfluidic channel whose height was 40 $\mu$m. Standard laser flow cytometry data for the same population of cells are shown in the *Insets* for comparison.

Because flow in the channel is laminar, we neither expect nor observe lateral motion of cells across the channel width. More than 60 devices have been tested and showed similar quantitative results, thus excluding irregularities of device fabrication.

To experimentally confirm that we are indeed differentiating cells based on their DNA content and not by size or volume ($G_0/G_1$ cells have half the DNA content of $G_2/M$ cells and are also smaller), we also measured and compared avian red blood cells (Accurate Scientific, Westbury, NY) with mammalian (sheep) red blood cells

(Sigma), both fixed with glutaraldehyde. Whereas avian red blood cells possess 2N DNA and are therefore in $G_0/G_1$ phase, mammalian red blood cells—the same 6- to 7-$\mu$m size as avian cells—contain no DNA. We observed capacitance peaks when avian cells flowed through our device, but we observed no significant peaks when interrogating the mammalian red blood cells—even after a series of experimental runs and measurements with a number of different devices. This confirms that we indeed are measuring DNA content rather than cell size or volume.

The avian red blood cells we measured have an average capacitance change, $\Delta C_T$, of 5.0 fF. Significant is the fact that avian red blood cells have less DNA content than SP2/0 cells and produce a smaller signal. Indeed, the ratio of observed signals of the two different types of cells (5.0–12.3 fF) is in remarkable quantitative agreement with the ratio of their DNA content [2.5 pg for *Gallus domesticus* vs. 6.1 pg for *Mus muscularis* (16, 17)].

To determine the exact relationship between capacitance, $\Delta C_T$, and DNA content, we plotted $\Delta C_T$ and DNA content for the different cell types measured. As shown in Fig. 4, there exists a strong linear dependence between the two at a frequency of 1 kHz.** This suggests that there may be a species-independent relationship between the DNA content of eukaryotic cells and the resulting change in capacitance as these cells transit in a low-frequency electric field. Because other cellular constituents may scale with DNA content (such as nuclear histones), we cannot be certain that the entirety of the capacitance signal is derived from DNA. However, the relationship between DNA content and $\Delta C_T$ holds across cells of the four species (yeast, mouse, rat, and human) that we sampled. Because it is unlikely that all of these species have the same stoichiometric relationship between DNA and other nuclear and cytoplasmic constituents, the most likely explanation for the linear relationship between DNA content and capacitance signal is that the latter is strictly a function of the former. On an operational basis, at least, the relationship appears to be sufficiently durable to allow prediction of DNA content on the basis of $\Delta C_T$.

Indeed, by using capacitance cytometry, we were able to detect progressive alterations in DNA content. Thus, Rat-1 rodent fibroblast cells were synchronized in the $G_0/G_1$ phase of the cell cycle by placing them in serum-depleted medium (containing 0.1% FBS) for 72 h. Subsequently, these cells again were permitted to grow in a serum-replete medium (containing 10% FBS). Aliquots of cells were harvested from the depleted medium and at intervals after the readdition of serum. Measurement of DNA content was performed by both capacitance cytometry (using a 40-$\mu$m-high channel) and by standard laser flow cytometry. A comparison of the histograms derived from capacitance cytometry and flow cytometry (Fig. 5) indicates that cells cultured in the depleted medium ($t$ = 0 h) are synchronized at a single value of $\Delta C_T$ (centered at 3.2 fF in the histogram), which represents $G_0/G_1$ phase. Twelve hours after the addition of serum, the DNA content of some cells has increased as they enter the S phase of the cell cycle. By 21 h, most of the cells are in the S phase and contain an amount of DNA between $G_0/G_1$ and $G_2/M$ phase. By 30 h, many of these cells have transited $G_2/M$ phase (centered at 6.4 fF), and by 48 h, the cell population once more has the appearance of an asynchronously growing population.

In summary, we describe a method of determining the DNA content of single eukaryotic cells—capacitance cytometry—that uses microelectrodes to measure changes in capacitance as cell-bearing fluid flows through a micrometer-sized channel. Of particular interest, we demonstrate a very tight and linear relationship between the capacitance and the DNA content of a cell, and we show that this relationship is *not* species-dependent (among yeast, mouse, rat, and human). That this relationship does not respect interspecies boundaries implies that the measurement $\Delta C_T$ is dependent on DNA content *per se* rather than on an associated cellular constituent that scales with the content of DNA.

DNA content analysis is a core technique in examining cellular physiology. We have demonstrated that our integrated microfluidic device can replicate the DNA histograms of standard laser flow cytometry. The potential applications of this simple and economical device are numerous, ranging from the experimental enumeration of DNA content in biological model systems to the determination of aneuploidy and proportion of S phase in clinical tumor samples. In addition to advantages in cost, size, robustness, and complexity, sample preparation for the device is quite simple, compared with laser-based flow cytometry. In the experiments reported here, cell samples were fixed in ethanol or glutaraldehyde, but such treatment is not necessary, thus opening the possibility of monitoring DNA content in living tissue, such as peripheral blood, sputum, or cerebrospinal fluid. This might be advantageous in tumor cell detection and in real-time monitoring of the effects of pharmacological agents on cell cycle and cell death. Capacitance cytometry is also uniquely suited to application in microchip-based cell sorting; current efforts in this area make use of external optical detectors (18, 19). The use of capacitance cytometry with these microchip-based cell sorters would reduce further the cost, size, and complexity of these devices.

**The ratio used to scale data taken with a 40-$\mu$m-high channel device was obtained by measuring mouse SP2/0 cells with both 30-$\mu$m- and 40-$\mu$m-high channel devices. The $G_0/G_1$ and $G_2/M$ peaks were centered at 3.75 fF and 7.50 fF, respectively, when cells were measured with a 40-$\mu$m-high channel device; this, in contrast to the $G_0/G_1$ and $G_2/M$ peaks, centered at 12.3 fF and 23.0 fF, respectively, when the same cells were measured with a 30-$\mu$m-high channel device.

We thank J. D. Carbeck for advising on the microfluidics and T. E. Shenk and J. Broach for providing the rat and yeast cells, respectively. In addition, we thank R. Fitzgerald, E. Olson, and D. Weitz for critical reading of this manuscript. O.A.S. acknowledges support from the Fannie and John Hertz Foundation. This work was supported in part by National Science Foundation Grant DMR 96-24536, a DuPont Young Faculty Award, and the NJ Commission on Science and Technology.

1. Ayliffe, H. E., Frazier, A. B. & Rabbitt, R. D. (1999) *IEEE J. Microelectromechanical Syst.* **8**, 50–57.
2. Huang, Y., Yang, J., Wang, X. B., Becker, F. F. & Gascoyne, P. R. C. (2000) *J. Hematother. Stem Cell Res.* **8**, 481–490.
3. Fromherz, P., Kiessling, V., Kottig, K. & Zeck, G. (1999) *Appl. Phys. A* **69**, 571–576.
4. Vassanelli, S. & Fromherz, P. (1997) *Appl. Phys. A* **65**, 85–88.
5. Maher, M. P., Pine, J., Wright, J. & Yu-Chong, Tai. (1999) *J. Neurosci. Methods* **87**, 45–56.
6. Kawana, A. (1996) in *Nanofabrication and Biosystems*, eds. Hoch, H. C., Jelinski, L. W. & Craighead, H. G. (Cambridge Univ. Press, Cambridge, U.K.), pp. 258–275 and references therein.
7. Jung, D. R., Cuttino, D. S., Pancrazio, J. J., Manos, P., Cluster, T., Sathanoori, R. S., Aloi, L. E., Coulombe, M. G., Czarnaski, M. A., Borkholder, D. A., *et al.* (1998) *J. Vac. Sci. Technol. A* **16**, 1183–1188.
8. Asami, K., Gheorghiu, E. & Yonezawa, T. (1999) *Biophys. J.* **76**, 3345–3348.
9. Polevaya, Y., Ermolina, I., Schlesinger, M., Ginzburg, B. Z. & Feldman, Y. (1999) *Biochim. Biophys. Acta* **15**, 257–271.
10. Pethig, R. (1979) in *Dielectric and Electronic Properties of Biological Materials* (Wiley, New York), pp. 1–376.
11. Takashima, S. (1963) *J. Mol. Biol.* **7**, 455–467.
12. Bone, S. & Small, C. A. (1995) *Biochim. Biophys. Acta* **1260**, 85–93.
13. Yang, L., Weerasinghe, S., Smith, P. E. & Pettitt, B. M. (1995) *Biophys. J.* **69**, 1519–1527.
14. Yen, A. (1989) in *Flow Cytometry: Advanced Research and Clinical Applications* (CRC, Boca Raton, FL).
15. Xia, Y., Kim, E. & Whitesides, G. M. (1996) *Chem. Mater.* **8**, 1558–1567.
16. Tiersch, T. R. & Wachtel, S. S. (1991) *J. Hered.* **82**, 363–368.
17. Greillhuber, J., Volleth, M. & Loidl, J. (1983) *J. Genet. Cytol.* **25**, 554–560.
18. Fu, A. Y., Spence, C., Scherer, A., Arnold, F. H. & Quake, S. R. (1999) *Nat. Biotechnol. (London)* **17**, 1109–1111.
19. Schrum, D. P., Culbertson, C. T., Jacobson, S. C. & Ramsey, J. M. (1999) *Anal. Chem.* **71**, 4173–4177.